A STUDYT ON AERODYNAMIC DESIGN INTEGRATION OF THE SUPERCRITICAL WING AND REAR-MOUNTED ENGINE CONFIGURATION

Zhidong Wang*,Meihong Zhang*,Junhong Wang *
***First Aircraft Design and Research Institute ,Shanghai, CHINA**

Keywords:*Supercritical Wing,Nacelle,Design Integration;*

Abstract

In This paper, a study is presented on the behavior of the aerodynamic interferences of rear-mounted engine to a supercritical wing and its impact on the aerodynamic characteristics of the aircraft at high-speed cruising with engine in several operations. The configuration studied is a civil regional aircraft for featuring a supercritical wing and rear-mounted high by代ass ratio turbofan engine with separate flow nacelle closely downstream. Numerical flow simulation based on CFD and verified by wind-tunnel tests is the major tool of this study .It is indicated that under certain conditions favorable interference exist on the above mentioned configuration which can be utilized to improve the cruise efficiency of the completed aircraft through effective optimal integrated design. Such an effective approach for the high-speed aerodynamic design integration of the supercritical wing and rear-mounted nacelle configuration is also presented here and demonstrated by numerical example.

1 Introduction

As we know, the behavior of the aerodynamics interference of engine to a wing has the large influence on the aerodynamic characteristics of a designed wing. If we could not meliorate it, the engine will not meet the flight performance, and handling quality of aircraft will become worse. In the primary designing of the regional jet aircraft of ARJ21, we have encountered this problem. Limited by some reasons of cabin layout and some other general configuration, the engine should be installed on the tail fuselage. We recognize that if not optimizing the position of the nacelle but mounting the engine on the rear fuselage will seriously inflect the aerodynamics character of engine nacelle and pylon by wing and the incoming stream of the engine. Sequentially the stream quality of the engine inlet will be worse and lift of the aircraft will decrease.

Based on these, in the detailed designing stage of ARJ21, a study of featuring a supercritical wing and rear-mounted high by pass ratio turbofan engine is performed, with numerical simulation using TFN model and TPS model. Then the integration of the fuselage and engine and the configuration of the engine to the supercritical wing are researched, which is presented in this paper.

2 Research of the phenomena of the interference of rear-mounted engine to supercritical wing in the wind-tunnel test

In 2001 and 2002, several series of testing have been done in China Aviation Aerodynamic Institute (Shenyang) Fl-2 Wind-Tunnel with the model of TFN on the tail fuselage to feature the interference influence of the lognitudinal position of the engine to the wing through lengthening the fuselage between the engine and wing. [1] N1 is defined as the original fuselage, and N2 is defined as lengthening the fuselage between the engine and wing by 80cm at the original fuselage, so does N3 by 160cm.

Table.1 shows the results of testing with the different fuselage as the mach number is 0.76, in here ΔC_l is defined as the lift coefficent of the fuselage(Wing-Body) with the engine detracting that of the fuselage(Wing-Body) without engine. Table.2 present the results as the mach number is 0.78.

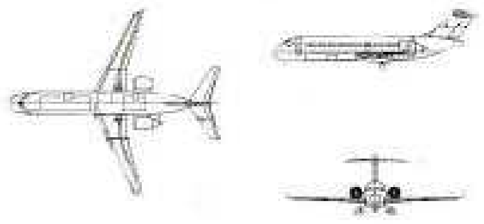

Fig.1.General arrangement

Table 1 m=0.76

α (deg)	fuselage	Δ Cl
0	N1	-0.08
	N3	-0.01`
2	N1	-0.08
	N3	-0.005
4	N1	-0.08
	N3	-0.005

Table 2 m=0.78

α (deg)	fuselage	Δ Cl
0	N1	-0.07
	N3	-0.01
2	N1	-0.07
	N3	-0.005

It is indicated that with the nacelle, lift coefficient decreased at the attacked angle of 0,2,4, and the lift coefficient of the aircraft with N1 fuselage decrease more than that of the N3 fuselage. Thus the less is the distance between the engine and wing, the more effect on the lift of the aircraft. Fig.2 shows the pressure distribution of the wing, which is clear that the incoming stream of the engine above the wing has depressed the stream on the wing, the intense of the shock wave decreased and the wave drag reduced.

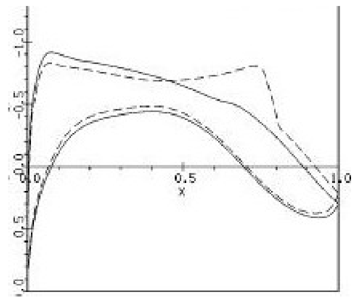

Fig.2. Comparing of Wing-Body and Wing-Body-Nacelle-Pylon C_p distribution across the wing on a section just before the nacelle

The same results are showed in Fig.3 as in the table.1 and table.2, that is, the engine nearer to wing the more wing lift lost. To our surprise, Fig.4 shows that comparing of the C_l-K chart of N2 and N3, the aerodynamic efficency K is similar when C_l is from 0 to 0.45. when C_l is over 0.45, the aerodynamic efficency of N2 position is much lower than that of N3 because lift lost, But , the aerodynamic efficency of N1 higher then both N2 and N3 which can be explained that drag decreased faster than that of the lift lost.That means there are beneficial interference of the rear-mounted engine to the supercritical wing as the configure of wing-mounted engine. At the same time, it is illuminated that when the aircraft is under cruising conditions, in which C_l is between 0.4~0.6, the aerodynamic efficiency of N1 position is better than other two installing positions. So N1 is defined as the feasible installing position of engine. But in fact, with position N1, as aerodynamic efficiency increases, the lift of aircraft has decreased. So it is no other than increasing the attacked angle of the aircraft to keep the aircraft flight with the 1g configure in cruising condition. On the other hand, while the flight angle is fixed, it is only by utilizing the beneficial interference to increase the aerodynamic efficiency. Then much more work should be done to optimize the installing position of the nacelle and redesigning the airfoil until the aerodynamic efficiency increase when the angle of attack is fixed.

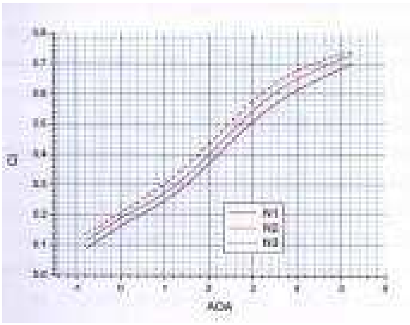

Fig.3.Variation of lift with angle of attack for three fuselage with and without nacelle

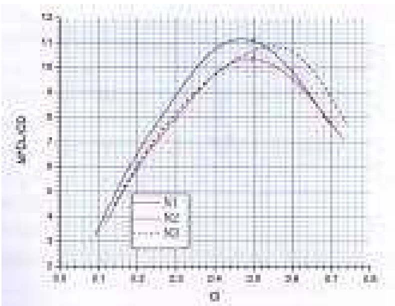

Fig.4.Variation of Aerodynamic Efficiency with Lift for three fuselage with and without nacelle

3 Integration of the rear-mounted engine to the supercritical wing

In the stage of integrating the rear-mounted engine to the supercritical wing, the wing airfoil is often designed by the aircraft company, which is based on the scheme of the general configuration, the designing requirement and guideline. On the other side, the engine must be designed based on the scheme of the general configuration and performance, too. So it is very important to meet the requirement of engine inlet at any flight condition as well as not to worsen the character of the wing pressure. All these work should be iterated many times.

3.1 Optimizing the installing position engine to the supercritical wing

From the above content, we know that if the lognitudinal position of the engine has been confirmed, the direction of the down stream of the wing must be calculated to minimize the drag of the wing. Constantly the area of the inlet of the engine must be kept as the largest, and because of the interference of the nacelle to the fuselage the transverse position of the engine should be taken into count, too, which is showed in Fig.5. The final result of the position in this area must be iterated by numerical method again and again, as following.

Fig.5.Propulsion system relative to aircraft centerline

Step 1, by calculating the flow field around the wing, especially at the installing position of the engine with the model of Wing-Body by N-S equation, we can catch the aerodynamic character in this field. Then we could get the pitch-up and toe-out angle of the engine installation position, which is showed in Fig.6 and Fig7.

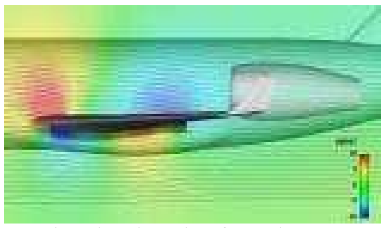

Fig.6.local angle of attack

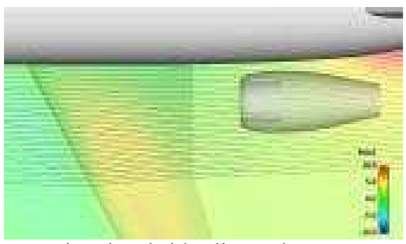

Fig.7.local side slip angle

Step 2, when the longitudinal position of nacelle is fixed, much trial work could be done of varying the nacelle positions in the set range until the installation position is the best. The movement and positions of nacelle are showed in Fig.8 and Fig.9.The basis of the selection are Mach number distribution on the nacelle and pylon. As we know, the peak mach number of

1.2 or below represents very small risk to drag, and peak Mach number above 1.4 represent higher risk to drag. So it is indicated from Fig. 10 that the position 0 and position 0a are well-behaved. The comparison of Mach number distribution of nacelle and pylon are showed in Fig.11 and Fig.12, which also indicated that the position 0a have the best Mach number distribution [2].

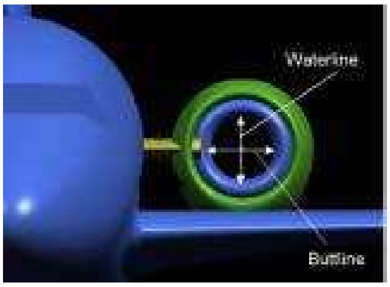

Fig.8.Movement of the nacelle
In waterline and buttline

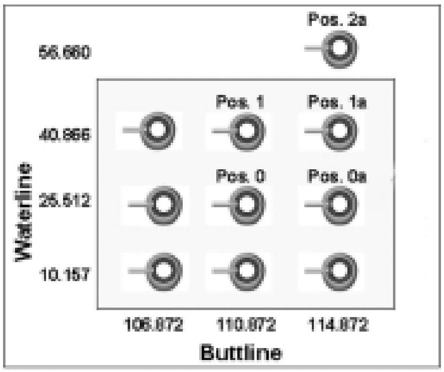

Fig.9.Variations of Nacelle扭position

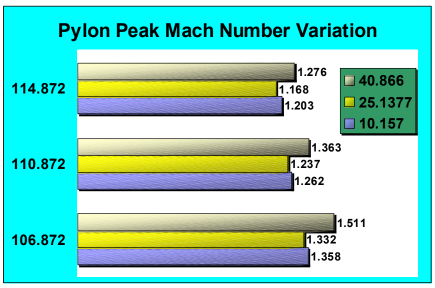

Fig.10.Waterline/Buttline study results

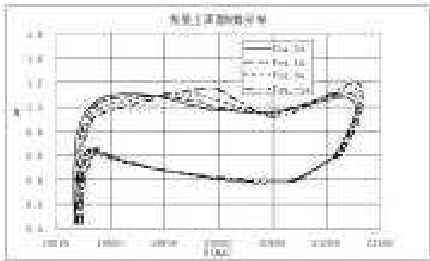

a. Upper Nacelle Mach Number distribution

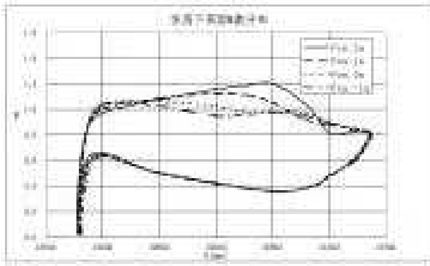

b. Lower Nacelle Mach Number distribution

Fig.11.Comparison of Mach number distribution of nacelle

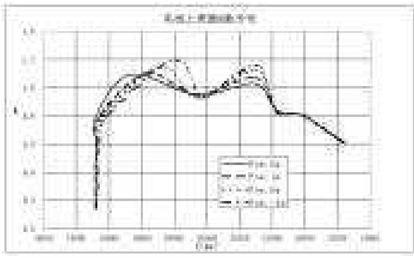

a. Upper Mid-Pylon Surface

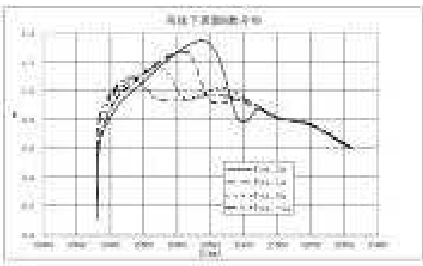

b. Lower Mid-Pylon Surface

Fig.12.Comparison of Mach number distribution of Mid-Pylon

3.2 The Wing modified designing

When the installing position of the engine has been confirmed at the rear fuselage, because the incoming stream has depressed the pressure on the wing trailing edge, the wing airfoil should be redesigned to increase the lift of the influenced wing. Two methods are used to redesign the airfoil, such as direct method and inverse method [3]. The direct method is to modify some dominate sections of the wing to meet the requirement. During redesigning the airfoil, considering the interference of the engine to the supercritical wing and the character of the supercritical wing, we modified some dominate sections with retaining the wing platform shape. From Fig.2, we could find that the interference of the engine to the wing has made the pressure distribution on the upper surface of the wing forward and downward, which lead to the lift coefficient decreasing and have little effect on the front of the wing and the lower surface of the wing. Thus through modifying the leading edge radius, thickness distribution, camber distribution, position of the maximum thickness, position of the maximum camber and the angle of the trailing edge will better the aerodynamics character of the wing, which is explained as following:

- Increasing the camber around the leading edge of the upper surface of the wing or increasing the radius of the leading edge to increase the lift coefficient.
- Increasing the camber of the trailing edge to increase the lift coefficient, but at the same time lead to the pitching moment increasing.
- Increasing chord wise extent of mid-wing may be relative to higher drag creep. By moving the position of the most thickness of the wing backward will get the position of the min pressure backward, which lead to the transition point backward, region of the laminar flow thicker, the turbulence flow shortening and the scrub drag decreasing.
- By moving the position of the most thickness of the wing backward also can lead to the position of the shock wave backward, make the separation slower and decrease the wave drag.

Besides these, to adjust the distribution of the torsion angle of the wing can make the circumfluence distribution airfoil like an ellipse, which reduce the induced drag.

Three dominate section airfoils of the new wing and the initial wing are compared in Fig.13, which is located at 25%, 35% and 44% of the whole wing. Fig.14 shows the different pressure distribution of both the modified and the initial wing.

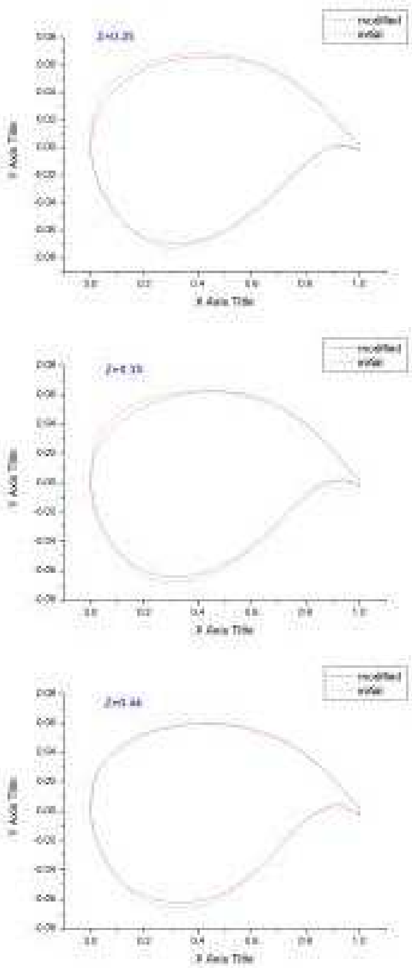

Fig 13.Comparison of original and modified wing cross-section

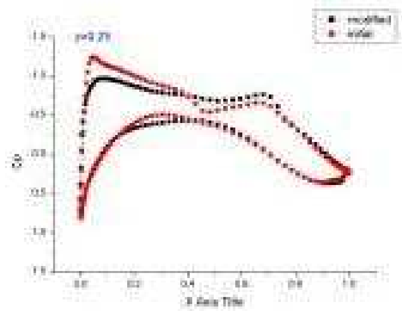

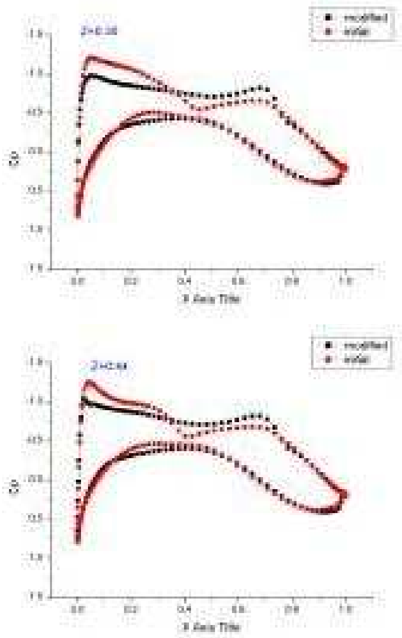

Fig 14.Ccomparison of C_p distribution of original and modified wing cross-section

The other method is that when the position of the nacelle has been confirmed, considering the interference of the engine to the wing, it is often used by custom-designing with existing airfoil design based on desired airfoil pressure distribution. But in this way, we need the computational program that can quickly calculate the flow around the model of the wing, fuselage, nacelle, pylon, such as the full potential equation method. In this stage, because all the section should be modified, much work should be done. And the desired pressure distribution shape must be scheduled by the person who is very experiential with the designing process.

Fig.15 shows an example of a designed wing. In this picture we could find out that favorable interference exist on the configuration which has been utilized by the designer when modifying the airfoil wing after optimizing the position of the nacelle. The pictures show that with the attacked angle increasing, the separated flow appears on the upper surface at the trailing edge of the inboard wing. But when the nacelle is installed above the wing, the separated flow disappeared, which tell us that the incoming flow of the engine has depressed the pressure of the wing with flowing slowly. The next figure 16 is the result of wind tunnel testing compared by the initial wing and the modified wing with nacelle. This illuminates that aerodynamic efficient has increased with the favorable interference of the engine. More modifying work of the wing or the nacelle should be done when moving the nacelle backward.

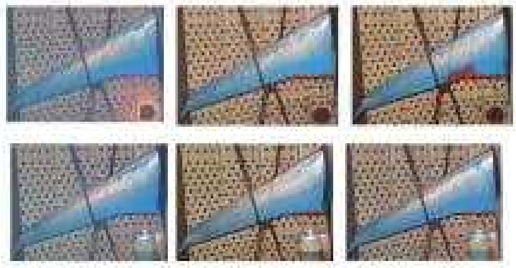

Fig.15. Test in T106 TsAGI wind tunnel,comparison oil flow visualization

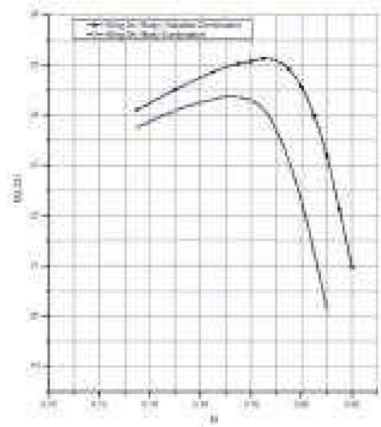

Fig.16.Test in T-106 TsAGI wind tunnel,comparison of Aerodynamic Efficiency with Mach number for wing-body and wing-body+nacelle-pylon

3.3 Verifying the position of the nacelle after modifying the wing airfoil

After modifying the wing airfoil ,in this step to verify the position of the nacelle by moving the nacelle backward or upward lightly with TFN model (the flow coefficient is 0.68), we could get some useful information.

First,compared by the lengthening the fuselage between the engine and wing, Lengthening the base fuselage by 38 inch and 76 inch,we get the mach number contours for mid-nacelle cut plane (Shown as Fig 17), Variation of lift with angle of attack for thre fuselarge configurations(Shown as Fig 18) and Variation of Aerodynamic Efficiency with Lift for three fuselarge configurations(Shown as Fig 19.)..It is possible to notice from these figures that the baseline nacelle position are well-behaved.

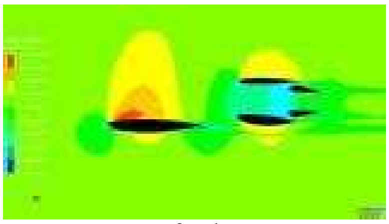

a Base fuselarge

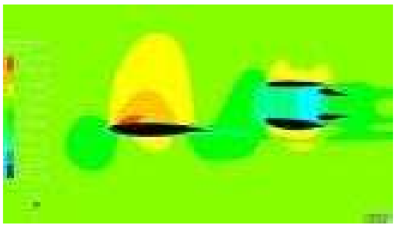

b fuselarge was stretched 38inch

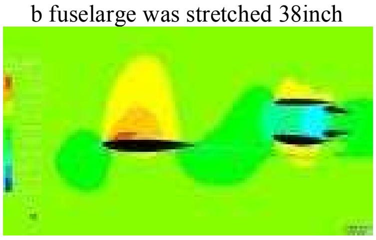

c fuselarge was starched 76inch

Fig.17.Mach number contours for mid-nacelle cut plane

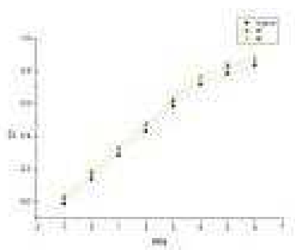

Fig.18.Variation of lift with angle of attack for thre fuselarge configuration

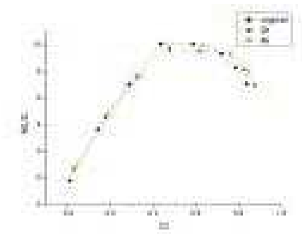

Fig.19.Variation of Aerodynamic Efficiency with Lift for three fuselarge configuration.

Then, Compared by raised nacelle position. raising the nacelle by 400 mm,we get another variation of Aerodynamic Efficiency with Lift for two configurations(shown in figure.20).which also indicated the baseline of nacelle position are well-behaved.

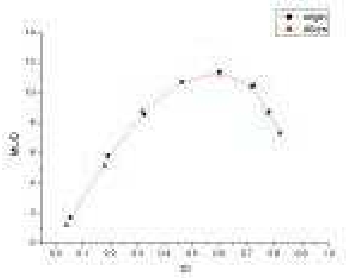

Fig.20.Variation of Aerodynamic Efficiency with Lift for two configuration

4 Powered nacelle used in non-designed condition

In the crusing condition, because the mass flow rato MFR of engine inlet is lower than 1.0,and the change of the MFR of the inlet to the influence on the pressure of the wing is not the most important. Thus using TFN technique in high speed wind tunnel test is a feasible and effective method. Besides these, we must also verify that at the other off-designed condition, the flow coefficient meet the requirement of the engine, such as APR, FIDL, Windmilling (as shown in Fig.21). So it is necessary to simulate the aerodynamic distribution include the inlet, fan duct and core duct air flow by the powered nacelle simulation.

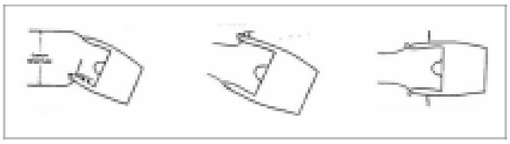

Low-speed windmilling high-speed cruising

Fig.21. The key status of the nacelle in the integration of the wing and nacelle

4.1 Geometry and Mesh

The geometry model is configured by CATIA5.10 .

The computations are performed with the Hexahedral meshes provided by ICEM-CFD to the commercial code CFX-5.

Te column flow field is applied, which radius is 10 times larger than the wing chord. The total meshes are about 3,500 thousand. According to our experience, the uneven meshes are distributed on the model. On the wing, thick mesh is arranged around the transition strips. And appropriate meshes on the nacelle, especially at the exits of the nacelle, shown as the following Fig.22and Fig. 23.

Fig.22 Overall meshes on the airplan

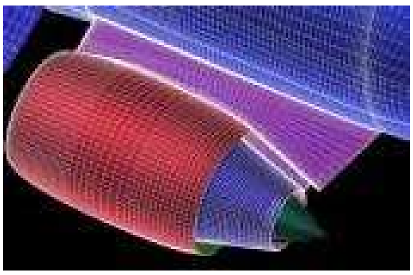

Fig.23.Grids on the nacelle from top viewing

4.2 Boundary condition and case condition

The boundary conditions [2][3] used in the present simulations are:

Inlet窠 pecified velocities and turbulence quantities (Tu=0.1%)

Walls栏 utomatic near-wall treatment (automatically switch from wall functions to a low-*Re* near wall formulation as the mesh is refined ($y+ < 0.2$))

Outlet-average static pressure to Mach number and Re number

Symmetry- 憁irror? the flow on either side of it. The normal velocity component at the Symmetry Plane boundary is set to zero, and the scalar variable gradients normal to the boundary are also set to zero.

Other-opening (for incoming flow freestream conditions, for outgoing flow static pressure)

Besides these, it is difficult set the nacelle CFD boundary. Flow into the fan face of the engine is modeled as flow EXIT in the CFX analysis. Similarly, the fan and core flows coming out of the engine at the aft end, as treated as flow SOURCES in the analysis, defining its total pressure and total temperature.

Case condition

- cruising condition
  Mach Number = 0.78, AOA =2.8 (degree)
  Air flow coefficient =0.71535
- APR case
  Mach Number = 0.43, AOA =3.5 (degree)
  Air flow coefficient =1.01913
- flight idle condition
  Mach Number = 0.82, AOA =1.0 (degree)
  Air flow coefficient =0.4111
- Windmilling case
  Mach Number = 0.43, AOA =3.5(degree)
  Air flow coefficient =0.33911

4.3 Numerical methed and results

The simulations are numerically based on the compressibleReynolds-Averaged Navier-Stokes equations. The equations are discretized using a vertex-based finite volume method, which is conservative and time-implicit. The Reynolds stresses in the momentum are computed using the SST (Shear-Stress Transport) two-equation turbulence model and an automatic wall treatment. The results are computed by time step iteration until they converged below $3.0*10^{-5}$.

The results(Mach number distribution at the plane of middle nacelle) are shown as the following Fig.31 to Fig.34,

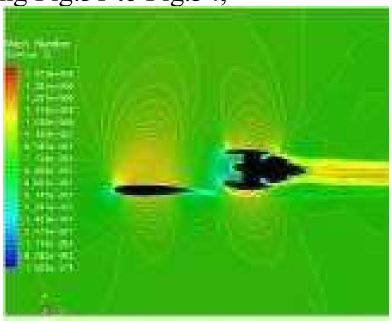

Fig.24. Mach number contours for mid-nacelle cut plane at cruising condition

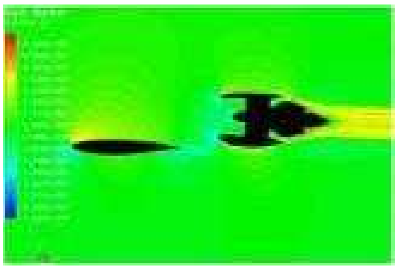

Fig.25. Mach number contours for mid-nacelle cut plane at APR condition

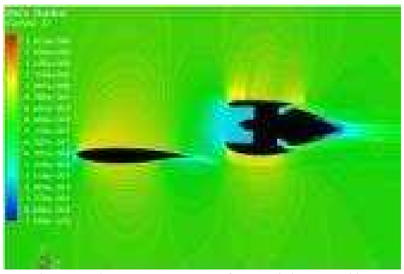

Fig.26. Mach number contours for mid-nacelle cut plane in FIDLING case

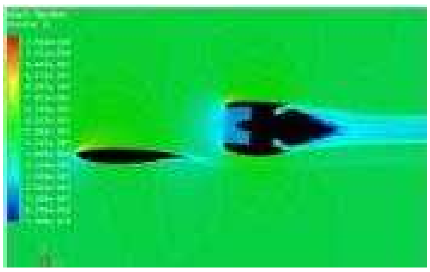

Fig.27. Mach number contours for mid-nacelle cut plane in Windmlling case.

Conclusion

In this paper,a methodology strongly based on CFD which is a tool used to identify the most promising configurations. But wind tunnel model tests are required to validate the final nacelle aerolines and installation concepts.

Acknowledgment

The authors wish to thank all partners and associated partners for their contribution to the program and for their permission to publish this paper.

References

[1] M F ling,K Peng.A feasibility study of the nacelle installation in wind tunnel FL-2. 2002 6,Report of ACAC of CHINA.

[2] GEAE,*ARJ21/CF34-10A Installation Study preliminary CFD Results,* SEP 2002.,Report of ACAC of CHINA.

[3] S Takanashi. *An iterative Procedure for Three Dimensional Transonic Wing Design by the Integral Equation Methed*, AIAA paper 84-2155

[4] Zhukovsky Center Aerohydrodynamic Institute(TsAGI), *Report on the results of testing the model of Chinese Regional Aircraft ARJ21 in the TsAGI's T-106 and T-128 Wind tunnel.* AUG 2004 .Report of FAI of CHINA.

[5] M H Zhang,Z D Wang. *Numerical Simulation of Powered nacelle in the integration of wing and rear-mounted nacelle East West High Speed Flow Field Conference.* Oct.19-22,2005 Beijing,China